

Dipole Charge Detection: Toward the Readout of Bistable Charge States in Molecular QCA

Mohammad Istiaque Rahaman , Gergo P. Szakmany , Alexei O. Orlov**, and Gregory L. Snider

Department of Electrical Engineering, University of Notre Dame, Notre Dame, IN 46556 USA

Manuscript received 30 June 2023; revised 8 September 2023 and 27 September 2023; accepted 28 September 2023. Date of publication 5 October 2023; date of current version 26 December 2023.

Abstract—Molecular electronics is one of the revolutionary platforms to perform computation. In molecular quantum-dot cellular automata (mQCA), binary information can be encoded in candidate molecules by single charge localization, and logic operation is performed by using electrostatic interactions among neighboring cells. However, charge detection at the molecular level is extremely challenging. In this letter, we have fabricated two isolated sub-20-nm metal dots interconnected by a tunnel barrier that mimics an mQCA cell. Using a novel charge cancelation scheme, we observe robust detection of electron switching in the double-dot structure by a single-electron transistor at a temperature of 2.7 K. The experimentally observed period of single-electron charging in the double dots is in good correlation with COMSOL multiphysics' simulations.

Index Terms—Sensor phenomena, molecular electronics, charge quantization, quantum-dot cellular automata (QCA), single-electron transistor (SET).

I. INTRODUCTION

Molecular electronics is a potential alternative to the field effect transistor-based paradigm, which is currently facing performance and reliability issues due to high-power dissipation, short-channel effects, etc. In molecular electronics, it is possible to perform a logic operation without any transistors. Quantum-dot cellular automata (QCA) is a promising transistorless computational paradigm [1], [2], where logic operations are performed by appropriate positioning of the QCA cells and their coulombic interaction between neighbor cells [3]. In molecular QCAs (mQCAs), one molecule works as a QCA cell. Electric field-driven bistability has been experimentally found in different candidate molecules, especially in mixed valance complex molecules for mQCA applications [4], [5], [6], [7]. However, to isolate a single molecule and sense its charge switching by an electrometer, this should be tackled first before performing any full-scale logic operation by these cells. In this context, the challenges of charge detection fidelity of a realistic electrometer in molecular regime are often overlooked.

Calculations performed by Blair and Lent [8] demonstrate that electron switching in molecular complexes is potentially detectable by using single-electron transistors (SETs) as charge sensors. However, experiments performed by Joyce et al. [9] yielded no detectable signal of the bistability of molecules by metallic SETs.

One of the primary challenges in detecting molecules using an SET is that both ends of the molecule are typically located at approximately the same distance from the detector, i.e., forming a dipole. As a result, when the localization of a single electron within a molecule switches, it tends to couple almost equally to the SET, resulting in hardly any

Corresponding author: Mohammad Istiaque Rahaman (e-mail: mrahaman@nd.edu).

Associate Editor: K. Shankar.

Digital Object Identifier 10.1109/LSENS.2023.3322265

measurable difference between the two states of the molecule. So, before attempting to detect field-driven bistability in mQCA cells, the detection experiment can be mimicked in sub-20-nm double-dot (DD) structures fabricated by high-resolution electron beam lithography (EBL) with two metal islands separated by a tunnel barrier. Here, the two dots work as redox sites in actual mQCA candidates where a single electron can be localized. The tunnel barrier is analogous to the bonded ligands in the real molecules, which connect two redox sites and facilitate discrete electron tunneling.

The use of SETs as electrometers for sensing charges is well established, starting with charge detection in a single-electron box (SEB) [10]. Charge detection of electron switching within metal DDs using SETs has been previously reported [11], [12], [13]. These previous works dealt with micron- and submicron-sized DD structures where each SET was essentially coupled to only one of the two dots so that the detection scheme was similar to the detection of electron charging in the SEB [10]. However, as previously mentioned, when the dot size shrinks, both of the dots tend to couple almost equally to the SET, which leads to little or no measurable voltage difference between the two charge states.

The purpose of this work is to perform controlled charge transfer between two sub-20-nm metal dots separated by a tunnel barrier and detect the transport of charge by metallic SETs. Hence, the design of the experiment needs to address two issues. First, in order to generate a measurable signal, it is necessary to ensure an asymmetry in the capacitive coupling from the two dots to the SETs. This reduces the mutual cancelation of signals that are associated with charge transfer in DD. This is particularly challenging when the size of the dots becomes comparable or even smaller than their distance to the detector. To achieve single-electron transfer, a high-voltage difference is needed across the DD. Yet, this voltage must be countered to avoid affecting the SET detector's working point.

Considering both, the charge detection fidelity of the SETs is pushed toward the ultimate limits of detection when the dot size shrinks

^{*}Member, IEEE

^{**}Senior Member, IEEE

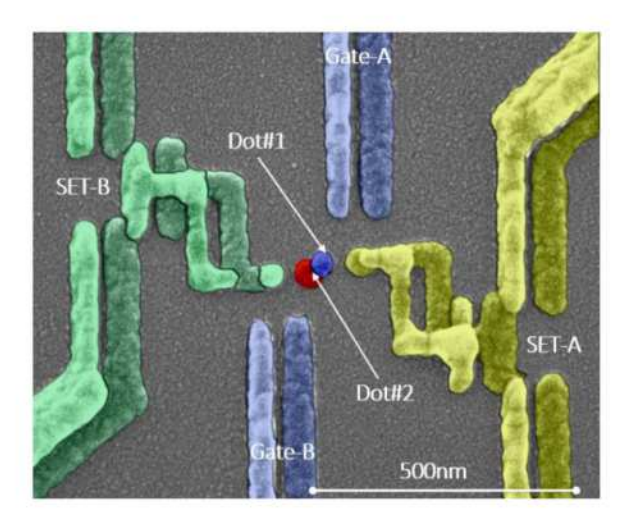


Fig. 1. Colorized scanning electron micrograph of the tested structure. Gate-A (purple) and gate-B (purple) control the electron tunneling from dot-1 (navy blue) to dot-2 (red) by application of common-mode bias. The SETs on the right (yellow) and on the left (green) are the electrometers. In the discussed experiments, SET-B was nonfunctional due to a fabrication defect.

toward that of the mQCA cell. Here, we provide an experimental demonstration of single charge transport between two aluminum dots and the detection of that transfer by aluminum SETs.

II. DEVICE FABRICATION AND MEASUREMENT

The devices are fabricated on a 700- μ m-thick fused silica substrate. The SET and DD patterns were exposed on polymethyl methacrylate (PMMA) 950 C2 with polymethylglutarimide (PMGI) SF-5 underneath on the substrate using a Raith EBPG 5200 100 keV EBL system. The electron beam exposed PMMA was developed using 3:1:1.5% of 2-propanol (IPA): methyl isobutyl ketone:methyl ethyl ketone. After that, a controlled undercut profile was created in PMGI by using metal ion-free tetramethyl-ammonium hydroxide photoresist developers. The aluminum SETs and DDs were fabricated in a thermal evaporator by Niemeyer-Dolan bridge shadow evaporation technique [14] with two layers of Al (20 and 40 nm) separated by a tunnel barrier obtained by in situ oxidation (7 μ Torr for 15 min).

After completing the device fabrication, the devices are wire bonded into a chip carrier and cooled to 2.7 K inside a pulsed tube H_e cryostat. The differential conductance $(G_{SET} = dI_{ds}/dV_{ds})$ of SETs is measured using a standard lock-in amplifier technique with ac probing voltage of 0.2 mV at 1.5-3.5 kHz. Fig. 1 shows the SEM micrograph of the device discussed in this work taken after the experiment.

We tested multiple device structures containing both SETs and observed "mutual detection" of the SETs in addition to the DD action. Specifically, we found that SET-A is detecting single-electron switching in SET-B and vice-versa. However, these results will be published elsewhere. For the experimental results discussed in the following text, SET-B is not functional (shows an open circuit) due to a fabrication defect, and only the signal from the DD is detected, thus simplifying the analysis.

III. RESULTS AND DISCUSSION

Fig. 2 represents a simplified circuit diagram of the experiment where the structure in the middle represents the two dots (red and blue)

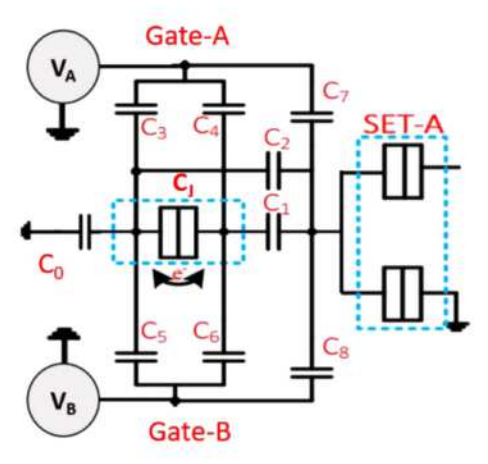


Fig. 2. Simplified circuit diagram of the experimental setup. Dashed blue line in the middle delineates the DD; the blue dashed line on the right delineates the detector SET-A. The capacitance values extracted from COMSOL multiphysics simulation are $C_1 = 1.62$ aF, $C_2 = 0.50$ aF, $C_3 = 0.41$ aF, $C_4 = 0.60$ aF, $C_5 = 0.79$ aF, $C_6 = 0.28$ aF, $C_7 = 7.3$ aF, $C_8 = 8.3$ aF, $C_0 \approx 0.9$ aF, and $C_j \approx 30$ aF for the barrier thickness

forming DD, as shown in Fig. 1. At low temperatures, $T < E_{Cd\Sigma}/k_B$, electrons are localized in the dots due to Coulomb blockade. Here, $E_{Cd\Sigma}$ is the charging energy of each dot in the DD structure and $C_{d\Sigma}$ is the total capacitance of each dot: $C_{d\Sigma 1} \approx C_{d\Sigma 2} = C_{d\Sigma}$, a reasonable assumption for a DD where the junction capacitance $C_J \gg C_i$ in Fig. 2; k_B is Boltzmann's constant. When differential voltage V_{Diff} is applied to the gates A and B (i.e., $V_{\mathrm{Gate-A}}$ is applied to gate A, and $V_{\mathrm{Gate-B}}$ is applied to gate B, where $V_{\mathrm{Gate-A}} \approx -V_{\mathrm{Gate-B}}$ and $V_{\mathrm{Diff}} = V_{\mathrm{Gate-B}}$ - $V_{\rm Gate-A} \approx 2 V_{\rm Gate-B}$), the Coulomb blockage in DD is overcome and electrons are transferred from left dot to the right dot with the period of $\Delta V_{\rm Diff} = e/C_{g{
m DD}}$, where $C_{g{
m DD}}$ is an equivalent coupling capacitance from DD to the gates. A SET coupled to DD with capacitances C_1 and C_2 experiences an induced charge [9]

$$\Delta q \propto \Delta V_{\rm DD} (C_1 - C_2)$$
 (1)

where $V_{\rm DD} = e/C_{d\Sigma}$ is the potential swing resulting from a singleelectron transfer in the DD at T=0. Finite temperature leads to a smearing of the abrupt sawtooth pattern and reduces its magnitude

The charging energy obtained from the charge stability diagram of SET-A (not shown) is $E_c \sim 0.75$ meV; this ensures significant peak-tovalley ratio ≈2 in Coulomb blockade oscillations (CBOs) at 2.7 K (blue trace in Fig. 3), which is necessary for the single-electron detection.

Turning now to the details of the experiment, SET must be biased at a sensitive position of its characteristics CBO [10] for detection of any nearby charge movement. If a single gate voltage (say, $V_{\text{Gate-A}}$) is applied across the DD, it also causes the shift of working point of SET-A because SET-A is directly coupled to Gate-A (see Fig. 1), thus completely masking a small signal resulting from the discrete charge transfer in the DDs.

In order to be able to detect the electron transfer in DD, we utilize a voltage cancelation scheme that differs from the "traditional" cancelation action [9], [10], [11], where an extra gate located close to the SET receives the appropriately scaled inverted signal from a DD gate. As can be seen from Fig. 1, the device structure in this work is designed to provide strong coupling from DD to the SET detectors while maintaining a maximal electric field across the DD. At the same time, coupling from both gates to each of the SETs is almost equal, thanks to the careful design of the structure layout. Therefore, if the

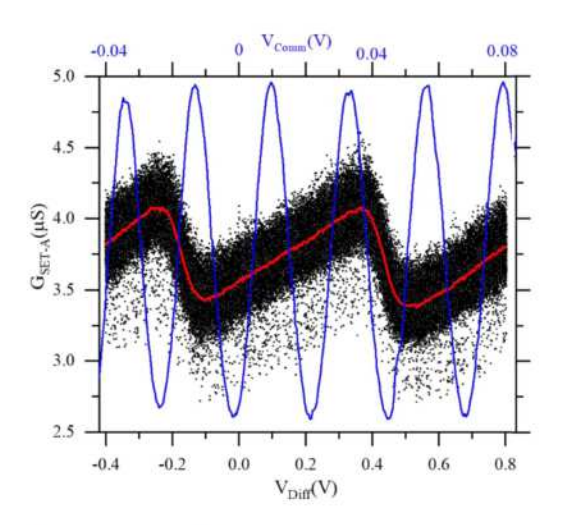


Fig. 3. Experimental results of detection of electron transition in DDs. Blue curve corresponds to the CBO of SET-A while varying both gates in parallel (i.e., $V_{\rm Gate-A} = V_{\rm Gate-B} = V_{\rm Comm}$). The black scatter plot is the raw data of conductance variations of SET-A for simultaneously biasing Gate-A and Gate-B, with voltage V_{Diff} in opposite directions $V_{\rm Diff} = V_{\rm Gate-B} - (-\alpha \cdot V_{\rm Gate-B})$, where $\alpha = 0.998$ (200 traces are presented). The red curve is the average of 200 consecutive scans. Set point is chosen in the middle of the rising slope of SET CBO.

differential voltage $V_{\rm Diff}$ is applied to Gates A and B (i.e., $V_{\rm Gate-A} =$ V_{Gate-B}), the SET-A is exposed to the same but opposing voltages. To cancel direct charge coupling from Gates A and B to SET-A, we slightly adjust the scaling coefficient α for the voltage applied to Gate-B: $V_{\text{Gate-A}} = -\alpha V_{\text{Gate-B}}$. The optimal cancelation is achieved when ramping the voltages of the opposite polarity causes no CBOs in the SET. The value of the scaling coefficient in Fig. 3 is $\alpha = 0.998$.

By choosing the working point in the middle of the raising slope of the SET electrometer response characteristic (blue trace in Fig. 3), we are able to detect small charge variations due to charge transfer in DD, which produces a measurable change in SET conductance. The period of characteristics sawtooth oscillations caused by singleelectron switching in the DD is found to be $\Delta V_{qDD} \approx 0.63 \text{ V}$.

We performed calculations of the capacitance matrix extracted for our device structure using the electrostatic module of COMSOL Multiphysics. To determine the capacitances between the various components of the structure, the electrostatics module of COMSOL Multiphysics was employed. The precise dimensions for the simulations were obtained from the SEM image (see Fig. 1) of the measured device. In the simulation, the SiO₂ substrate and air were represented by two hemispheres with relative permittivities of 3.9 and 1, respectively. The Al₂O₃ tunnel barrier was incorporated between the two dots, with a relative permittivity of 9.5. By utilizing a parametric sweep for each component, COMSOL calculated the mutual capacitance matrix, and the relevant capacitance values were subsequently extracted. The calculated capacitance values are listed in the caption of Fig. 2.

The voltage distribution map across the structure for a differential bias $V_{\rm Diff} = 2$ V for the extracted capacitances is plotted in Fig. 4. It is clear that the potential gradient is the strongest along the DD structure. Based on the simulations of the coupling capacitances from Gate-A and Gate-B to DD, the expected voltage required for a transfer of a single electron between the two dots is ≈ 0.6 V, assuming the capacitance $C_j \approx 30$ aF, in reasonable agreement with the observed value of ≈ 0.63 V.

Simulations confirm that the coupling capacitances to SET-A for two dots in Fig. 1 are noticeably different, $C_1 = 1.62$ aF and $C_2 =$

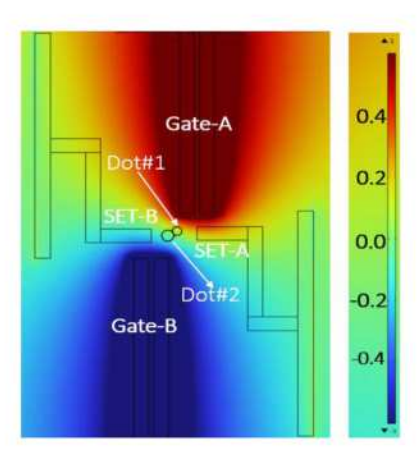


Fig. 4. COMSOL Multiphysics simulation of test structure, as shown in Fig. 1. Gate-A biased at +1 V and gate-B biased at -1 V. The color bar shows the potential distribution across the structure.

0.5 aF, respectively. This difference was significant enough for the SET to detect electron transitions inside the DDs. For a single-electron charging in a DD, the induced charge on SET-A due to a single-electron transition between the dots is calculated to be $\Delta q = 0.078e$ at the temperature of the experiment, 2.7 K. This value is extracted from the equivalent conductance change in calibration curve (blue trace in Fig. 3) equal to conductance swing caused by the single-electron transition in the DD [10]. Note that our experiment is performed at a temperature that is about two orders of magnitude higher than previously reported DD detection results [11], [12].

Finally, the metallic DDs can be considered as prototypes for real candidate molecules in the context of mQCA applications, with the exception of experimentally synthesized [16] and proposed [17], [18] molecules that are sub-1-nm in size. For a comprehensive understanding of single charge transport at the molecular level, SETs emerge as an optimal choice due to their unparalleled charge sensitivity, capable of detecting changes equivalent to a fraction of a single charge. Even minute alterations in charge distribution in the proximity of the SETs are amplified by their steep CBO slope, resulting in a measurable change in conductance. Therefore, as long as SETs are strategically positioned around the candidate molecules to create a difference in coupling capacitance ($C1 \neq C2$, as depicted in Fig. 2), our proposed cancelation scheme ensures detectable conductance changes in SETs, enabling the detection of charge transfer.

Furthermore, our experimental prototype of candidate mQCA molecules can potentially be detected through radio frequency gate (RFGate) reflectometry [19] and tip-enhanced Raman spectroscopy techniques [11]. While the effectiveness of these alternative detection methods in the context of DD sensing is intriguing, it lies outside the immediate scope of this current study. We are actively involved in further research involving RFGate reflectometry applied to our DDs, which will serve as the central focus of our forthcoming publication dedicated to the exploration of charge transport in the sub-20-nm regime.

IV. CONCLUSION

Discrete charge quantization in sub-20-nm metal DDs separated by a tunnel barrier has been observed at T = 2.7 K using metal-oxide SETs, mimicking the charge transport in candidate molecules suitable for mQCA. We employed a charge cancelation scheme that automatically neutralizes the differential bias responsible for single-electron transfer between the dots in the DD "molecule" through the strategic placement of the sensing SET electrometer.

ACKNOWLEDGMENT

This work was supported by U.S. National Science Foundation under Grant DMR-1904610.

REFERENCES

- C. S. Lent and P. D. Tougaw, "A device architecture for computing with quantum dots," *Proc. IEEE*, vol. 85, no. 4, pp. 541–557, Apr. 1997.
- [2] A. O. Orlov, I. Amlani, G. H. Bernstein, C. S. Lent, and G. L. Snider, "Realization of a functional cell for quantum-dot cellular automata," *Science*, vol. 277, pp. 928–930, Aug. 1997.
- [3] A. Islamshah, A. O. Orlov, G. Toth, G. H. Bernstein, C. S. Lent, and G. L. Snider, "Digital logic gate using quantum-dot cellular automata," *Science*, vol. 284, no. 5412, pp. 289–291, 1999.
- [4] Q. Hua et al., "Molecular quantum cellular automata cells: Electric field driven switching of a silicon surface bound array of vertically oriented two-dot molecular quantum cellular automata," J. Amer. Chem. Soc., vol. 125, no. 49, pp. 15250–15259, 2003.
- [5] C. S. Lent, B. Isaksen, and M. Lieberman, "Molecular quantum-dot cellular automata," J. Amer. Chem. Soc., vol. 125, no. 4, pp. 1056–1063, 2003.
- [6] R. M. Macrae, "Mixed-valence realizations of quantum dot cellular automata," J. Phys. Chem. Solids, vol. 177, 2023, Art. no. 111303.
- [7] Y. Ardesi, A. Pulimeno, M. Graziano, F. Riente, and G. Piccinini, "Effectiveness of molecules for quantum cellular automata as computing devices," J. Low Power Electron. Appl., vol. 8, no. 3, 2018, Art. no. 24.
- [8] E. P. Blair and C. S. Lent, "Quantum-dot cellular automata: An architecture for molecular computing," in *Proc. Int. Conf. Simul. Semicond. Processes Devices*, 2003, pp. 14–18.

- [9] R. A. Joyce, H. Qi, T. P. Fehlner, C. S. Lent, A. O. Orlov, and G. L. Snider, "A system to demonstrate the bistability in molecules for application in a molecular QCA cell," in *Proc. IEEE Nanotechnol. Mater. Devices Conf.*, 2009, pp. 46–49.
- [10] P. H. Lafarge, H. Pothier, E. R. Williams, D. Esteve, C. Urbina, and M. H. Devoret, "Direct observation of macroscopic charge quantization," *Zeitschrift fur Physik B Condens. Matter*, vol. 85, pp. 327–332, 1991.
- [11] I. Amlani, A. O. Orlov, R. K. Kummamuru, G. H. Bernstein, C. S. Lent, and G. L. Snider, "Experimental demonstration of a leadless quantum-dot cellular automata cell," *Appl. Phys. Lett.*, vol. 77, no. 5, pp. 738–740, 2000.
- [12] T. M. Buehler, D. J. Reilly, R. Brenner, A. R. Hamilton, A. S. Dzurak, and R. Clark, "Correlated charge detection for readout of a solid-state quantum computer," *Appl. Phys. Lett.*, vol. 82, no. 4, pp. 577–579, 2003.
- [13] T. M. Buehler et al., "Development and operation of the twin radio frequency single electron transistor for cross-correlated charge detection," J. Appl. Phys., vol. 96, no. 8, pp. 4508–4513, 2004.
- [14] T. A. Fulton and G. J. Dolan, "Observation of single-electron charging effects in small tunnel junctions," *Phys. Rev. Lett.*, vol. 59, no. 1, 1987, Art. no. 109.
- [15] C. W. J. Beenakker, "Theory of Coulomb-blockade oscillations in the conductance of a quantum dot," Phys. Rev. B, vol. 44, no. 4, 1991, Art. no. 1646.
- [16] J. Christie et al., "Synthesis of a neutral mixed-valence diferrocenylcarborane for molecular quantum-dot cellular automata applications," *Angewandte Chemie*, vol. 127, pp. 15668–15671, 2015.
- [17] N. Liza, D. Murphey, P. Cong, D. W. Beggs, Y. Lu, and E. P. Blair, "Asymmetric, mixed-valence molecules for spectroscopic readout of quantum-dot cellular automata," *Nanotechnology*, vol. 33, no. 11, 2021, Art. no. 115201.
- [18] X. Wang, L. Yu, V. S. S. Inakollu, X. Pan, J. Ma, and H. Yu, "Molecular quantum dot cellular automata based on diboryl monoradical anions," J. Phys. Chem. C, vol. 122, no. 4, pp. 2454–2460, 2018.
- [19] M. J. Filmer et al., "Gate reflectometry of single-electron box arrays using calibrated low temperature matching networks," Sci. Rep., vol. 12, no. 1, Feb. 2022, Art. no. 3098.